Model nonlinear block copolymers: Synthesis, Characterization, Morphology

N. Hadjichristidis[a]; Y. Tselikas[a]; H. Iatrou[a]; V. Efstratiadis[a]; A. Avgeropoylos[a]

[a] Department of Chemistry, University of Athens Panepistimiopolis, Athens, Zografou, Greece

PLEASE SCROLL DOWN FOR ARTICLE

MODEL NONLINEAR BLOCK COPOLYMERS: SYNTHESIS, CHARACTERIZATION, MORPHOLOGY

N. HADJICHRISTIDIS,* Y. TSELIKAS, H. IATROU,
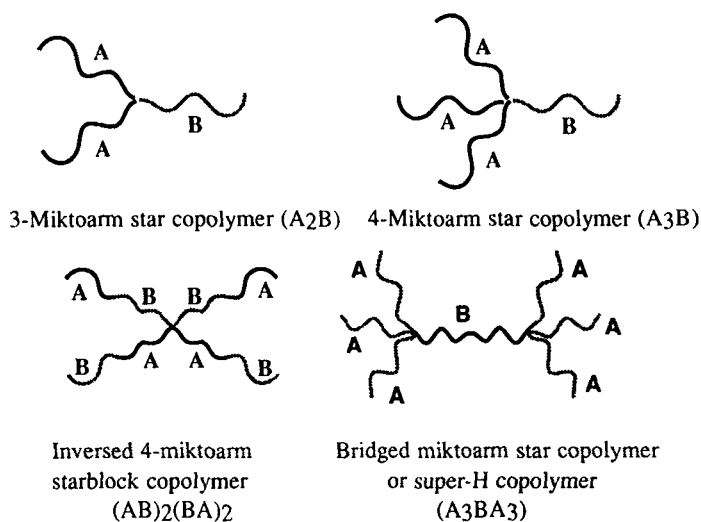V. EFSTRATIADIS, and A. AVGEROPOYLOS

Department of Chemistry
University of Athens
Panepistimiopolis, Zografou, 157 71 Athens, Greece

ABSTRACT

The synthesis of well-defined, near monodisperse, nonlinear block copolymers of the A_2B (3-miktoarm star copolymers), A_3B (4-miktoarm star copolymers), $(AB)_2(BA)_2$ (inversed 4-miktoarm star block copolymers), and A_3BA_3 (bridged miktoarm star copolymers) types is described. A is polyisoprene (PI) and B is polystyrene (PS). The synthetic approach involves the reaction of methyltrichlorosilane or tetrachlorosilane with monofunctional or difunctional macroanions of B under conditions unfavorable to chain coupling or linking, followed by addition of the monofunctional macroanion A. Characterization was carried out by size exclusion chromatography, low-angle laser light scattering, laser differential refractometry, membrane and vapor pressure osmometry, and NMR and UV spectroscopy. Microphase separation was studied by transmission electron microscopy and small-angle x-ray scattering. Comparison with the corresponding linear block copolymers showed that the macromolecular architecture not only strongly affects the morphological domain borders but can introduce new morphologies as well.

INTRODUCTION

The design and synthesis of well-defined and nearly monodisperse nonlinear block copolymers is of great interest since it allows investigation of the influence of chain architecture on properties. Miktoarm (mikto from the Greek word μικτός,

3-Miktoarm star copolymer (A2B)   4-Miktoarm star copolymer (A3B)

Inversed 4-miktoarm
starblock copolymer
(AB)2(BA)2

Bridged miktoarm star copolymer
or *super-H copolymer*
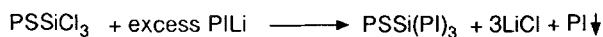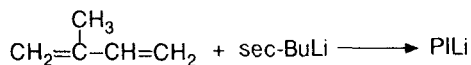(A3BA3)

SCHEME 1.   Nonlinear block copolymers.

meaning mixed) star polymers, which are star polymers with chemically different
arms, and bridged miktoarm star polymers (Scheme 1) are a few examples of
nonlinear block copolymers.

These new materials provided the necessary materials for morphological stud-
ies (TEM, SAXS, Image Simulation) which aim to reveal the influence of macromo-
lecular architecture on the structure of microphase-separated block copolymers.

SYNTHESIS AND CHARACTERIZATION

The synthesis of the nonlinear block copolymers was based on anionic poly-
merization and chlorosilane chemistry using standard high vacuum techniques. In
this approach, the reaction of methyltrichlorosilane or tetrachlorosilane with mono-
functional (in the case of star polymers) or difunctional (in the case of bridged
polymers) macroanions of B was carried out under conditions that allow the con-
trolled substitution of the desired number of chlorine atoms by the macromolecular
chains. In a second step the monofunctional macroanion A was added.

For example, the basic reactions used for the synthesis of 4-miktoarm star
copolymers of the A_3B type [1] are the following:

$$CH_2{=}CH \ + \ \text{sec-BuLi} \longrightarrow PSLi$$

$$PSLi \ + \ \text{excess} \ SiCl_4 \longrightarrow PSSiCl_3 \ + LiCl + SiCl_4{\uparrow}$$

$$CH_2{=}\overset{CH_3}{\underset{}{C}}{-}CH{=}CH_2 \ + \ \text{sec-BuLi} \longrightarrow PILi$$

$$PSSiCl_3 \ + \text{excess} \ PILi \longrightarrow PSSi(PI)_3 \ + 3LiCl + PI{\downarrow}$$
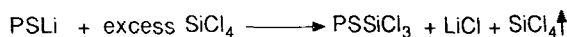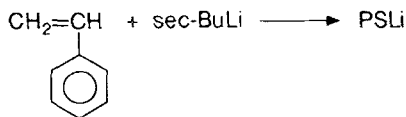
The excess of PILi after neutralization with methanol is removed by fractionation. For the synthesis of the A_2B stars [2], CH_3SiCl_3 was used instead of $SiCl_4$.

In Table 1 the molecular characteristics of a few A_2B and A_3B miktoarm star copolymers are given. It is clear that these copolymers are model compounds with a high molecular and compositional homogeneity. This fact is also supported by the excellent agreement between the compositions of the miktoarm copolymers calculated from the M_n of the arms and the ones found by UV and NMR.

Another type of miktoarm stars prepared using the chlorosilane approach is the inversed miktoarm starblock copolymers (Scheme 1). The basic reactions for the synthesis are the following [3]:

$$CH_2{=}\overset{\overset{\displaystyle CH_3}{|}}{C}{-}CH{=}CH_2 + \text{sec BuLi} \longrightarrow \text{PILi} \xrightarrow[\text{Styrene}]{\text{THF(small quantity)}} \text{(PI-b-PS)Li}$$

$$2(\text{PI-b-PS})\text{Li (small excess)} + SiCl_4 \xrightarrow{\text{titration}} (\text{PI-b-PS})_2SiCl_2 + 2LiCl$$

$$CH_2{=}\underset{\underset{\bigcirc\!\!\!\!\!\!\bigcirc}{\displaystyle \bigcirc}}{CH} + \text{sec BuLi} \longrightarrow \text{PSLi} \xrightarrow{\text{Isoprene}} \text{(PS-b-PI)Li}$$

$$(\text{PI-b-PS})_2SiCl_2 + \text{excess (PS-b-PI)Li} \longrightarrow$$

$$(\text{PI-b-PS})_2Si(\text{PI-b-PS})_2 + 2LiCl + \text{PS-b-PI}$$
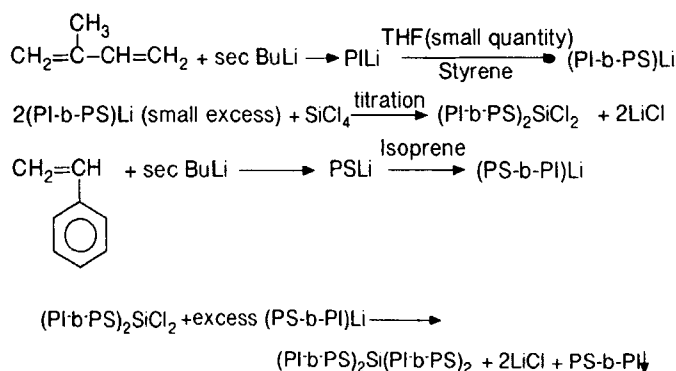
During the synthesis of the (PI-*block*-PS)Li living diblock, a small amount of THF was added in order to increase the reactivity of the polyisoprenyllithium anion toward styrene initiation. Thus, the styrene polymerization has a fast initiation step and the narrow distribution of the (PI-*block*-PS)Li arm is ensured.

The titration step was monitored by size exclusion chromatography (SEC). SEC chromatograms of the precursors along with the ones taken during the synthesis and those of the raw product and of the fractionated inverse starblock copolymer

TABLE 1. Molecular Characteristics of 3- and 4-Miktoarm Star Copolymers of the A_2B and A_3B Type[a]

Sample	$M_n \times 10^{-3}$			$M_w \times 10^{-3}$, Star	I, Star
	PS	PI	Star		
$PS(PI)_2$	21.7	19.9	50.3	53.4	1.05
$(PS)_2PI$	20.8	33.8	70.4	75.3	1.05
$PS(PI)_3$	35.2	14.5	77.2	80.1	1.05
$PS(PI)_3$	180	7.6	199	204	1.03

[a]$I = M_w/M_n$. Polydispersity index determined by SEC.

are shown in Fig. 1. The molecular characteristics of the inverse starblocks (ISB) given in Table 2 indicate a high degree of homogeneity.

For the synthesis of the A_3BA_3 type, the following reaction scheme was followed [4]:

napthalene + Na $\longrightarrow$ sodium napthalenide (I)

St (or Is) + (I) $\longrightarrow$ NaPSNa (or NaPINa)   (II)

(II) + excess $SiCl_4$ $\longrightarrow$ $Cl_3SiPSSiCl_3$ (or $Cl_3SiPISiCl_3$) (III)

(III) + excess PILi (or PSLi) $\longrightarrow$ $(PI)_3PS(PI)_3$ (or $(PS)_3PI(PS)_3$)
$$+ PI\!\downarrow \text{ (or } PS\!\downarrow\text{)}$$
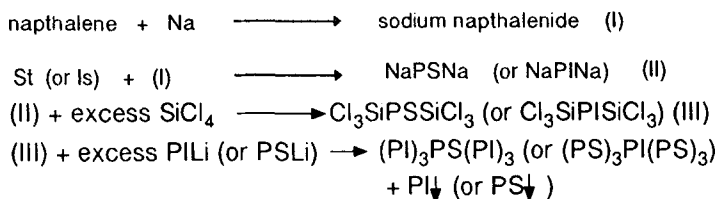
The living difunctional polymer, prepared by the procedure described by Roovers and Toporowski [5], is added to a very large excess of $SiCl_4$ to obtain the bridging
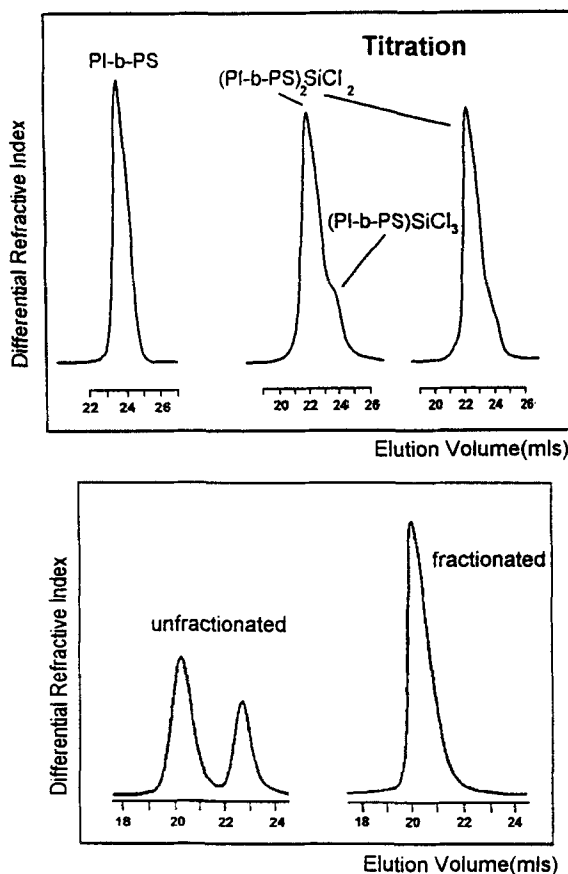

FIG. 1.   SEC chromatograms taken during the different stages of the synthesis of the inverse starblock copolymer.

TABLE 2.   Molecular Characteristics of Inverse
Starblock Copolymers

Sample	SB1	SB2	SB3
$M_n(PS) \times 10^{-3}$	82.0	36.1	20.0
$M_n(PS\text{-}block\text{-}PI) \times 10^{-3}$	101	52.6	37.3
PS wt% content:			
UV-SEC	80	65	49
^{1}H NMR	80	68	48
$M_n(PI) \times 10^{-3}$	73.0	32.5	17.9
$M_n(PI\text{-}block\text{-}PS) \times 10^{-3}$	93.1	50.0	37.4
PS wt% content:			
UV-SEC	20	35	50
^{1}H NMR	21	37	51
$M_n(star) \times 10^{-3}$	378	212	148
$M_w(star) \times 10^{-3}$	395	220	152
$I(star)$ (SEC)	1.05	1.04	1.03
PS wt% content:			
UV-SEC	48	50	49
^{1}H NMR	50	49	49
dn/dc	53	51	51
Calculated	50	51	50
Asymmetry parameter a	4	2	1

polymer chain (or connector) functionalized at both ends with the $-SiCl_3$ group. Addition of an excess of living polymer of the branches leads to the super-H copolymer (H-shaped copolymer; from the similarity to the letter H; super-H-shaped by analogy). The molecular characteristics (Table 3 indicate a high degree of molecular and compositional homogeneity.

TABLE 3.   Molecular Characteristics of the Super-H-Shaped Block
Copolymers[a]

	$M_n \times 10^{-4}$			$M_w \times 10^{-4}$,	I,	wt% PS	
Sample	Connector	Arm	SH	SH	SH	M_n	NMR
$(PS)_3PI(PS)_3$	2.19	0.4	4.56	4.62	1.08	52	51
$(PI)_3PS(PI)_3$	10.9	1.61	20.9	22.5	1.08	53	52
$(PI)_3PS(PI)_3$	10.9	2.94	29.0	30.8	1.07	38	37

[a]$I = M_w/M_n$. Polydispersity index determined by SEC.

MORPHOLOGY

It is generally accepted that the equilibrium morphology of block copolymers is governed by four factors: the Flory–Huggins interaction parameter χ, which describes the interactions between the two different polymer segments; the number of statistical segments in the polymer chain N; the volume composition ϕ; and the macromolecular architecture [6, 7].

The morphology of these new model nonlinear block copolymers was examined mainly by TEM and image simulation and checked by SAXS. By comparing the observed morphologies for the A_2B [8] and A_3B [9] miktoarm stars with the linear diblocks, it is clear that architecture significantly influences the microdomain structure at a given volume fraction (Fig. 2).

It is characteristic that in the case of 50% PS, the linear diblocks form lamellae while the $(PI)_2PS$ miktoarm star has a bicontinuous cubic structure and the $(PI)_3PS$ miktoarm forms hexagonally packed cylinders of PS in a PI matrix. TEM micrograms demonstrating this behavior are shown in Fig. 3. It is generally observed that the phase diagram in the strong segregation limit (SSL) for diblocks is shifted toward higher volume fractions of PS when PS is the single arm B in the A_nB miktoarm star. The amount of this shift depends on n, the number of A chains connected at the star center.

An important characteristic of A_3B morphology is that the spherical morphology is no longer observed at a high B volume fraction. Specifically, the $(PI)_3PS$ sample containing 92 vol% PS shows order only on a local scale (Fig. 4a). The sample consists of PI cylinders in a PS matrix, but the hexagonal orientation of the cylinders is maintained only locally. At this volume fraction the sample is near the order–disorder transition, and spherical morphology should appear as it does in the case of linear diblocks. Due to the high PS content, it is safe to assume that the spherical morphology has been completely eliminated from the phase diagram of
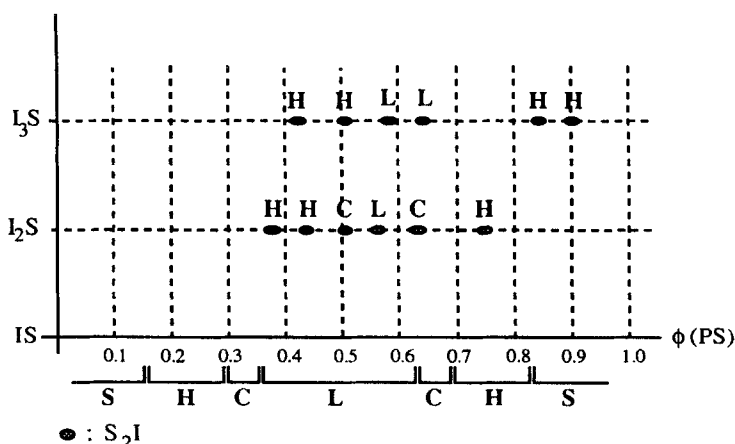

FIG. 2.   Observed morphologies of I_2S and I_3S miktoarm stars having various volume fractions of PS. Comparison with the linear block copolymers. S: bcc spheres. H: hexagonal cylinders. C: bicontinuous cubic. L: lamellae.
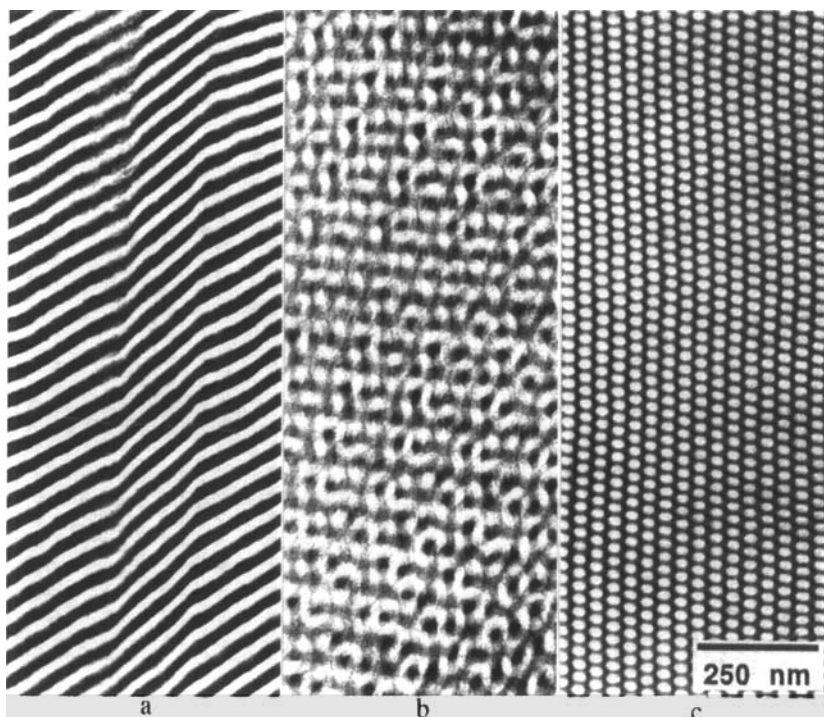
FIG. 3.   TEM micrograms of (a) a PI–PS diblock copolymer, (b) a $(PI)_2PS$ miktoarm star, and (c) a $(PI)_3PS$ miktoarm star, all having ~50 vol % PS.

such miktoarm stars. The sample containing 85 vol% PS exhibits a well-ordered hexagonally packed cylindrical morphology (Fig. 4b).

The above-mentioned behavior can be explained in terms of the local preferred curvature of the A–B interface as shown in Fig. 5.

Due to overcrowding of the A chains, the interface is forced to curve toward the B side. The more A chains are forced to occupy the same area of the interface, the more it curves in order to provide the necessary space for the A chains to pack without severe energy penalties due to chain stretching. The curving of the interface indicates the morphology which the system will finally adopt. The interfacial energy increases as the size of the interface increases. For a symmetric block copolymer of any architecture, the interfacial energy becomes a minimum when the interface is flat. Curving of the interface at 50% composition results in an increase in interface area, and therefore a relative energy penalty arises for the system. On the other hand, overcrowding near the interface causes the A chains to stretch away from it. The stretching energy is the free energy increment which the molecule suffers as it moves away from its unperturbed dimensions. The resulting morphology of the system is determined by a delicate balance between the interfacial energy (which is the enthalpic term in the free energy expression) and the stretching energy (which describes the entropic term in free energy).

The theoretical approach of Milner [10] has been developed in order to predict the structure of these miktoarm copolymer microphases at the SSL. This treatment
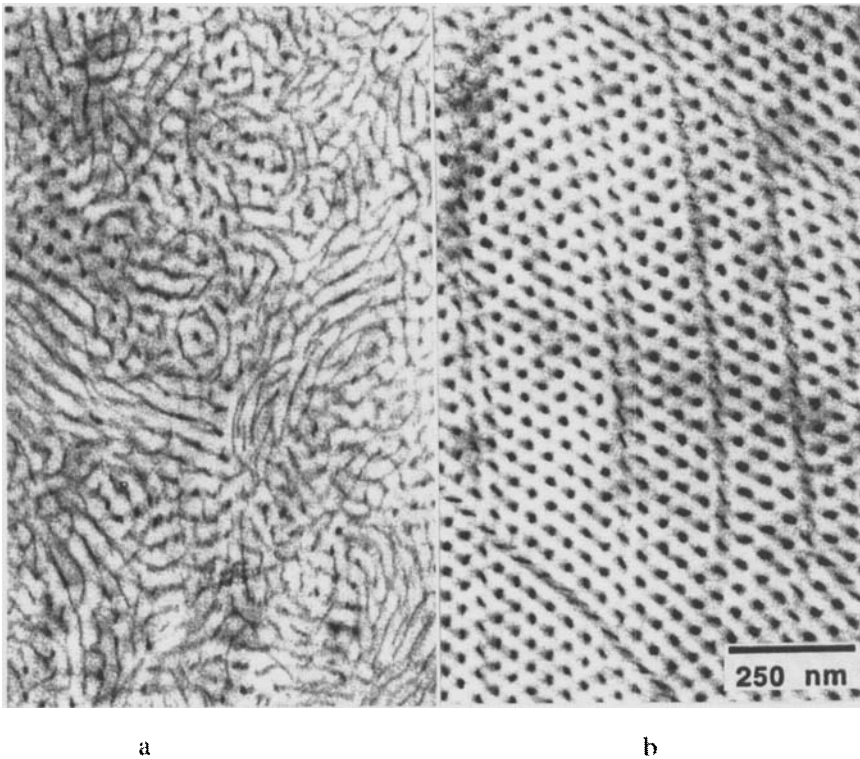
a   b

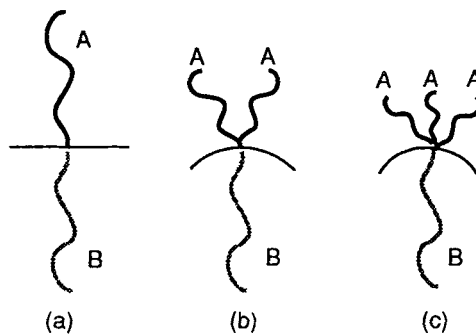FIG. 4.   TEM micrograms of A_3b miktoarm stars having (a) 92 vol% PS and (b) 85 vol% PS.

(a)   (b)   (c)

FIG. 5.   Model for different interfacial curvatures for (a) AB, (b) A_2B, and (c) A_3B copolymers with the same 50% composition. The greater crowding on the A side of the interface for the miktoarm case leads to a higher degree of curvature.

involves calculations of the chain free energies. In the case of A_nB miktoarms, the A side of the interface contains n times as many chains per unit area as the B side, so the A arms are much more strongly stretched than the B chains. The total free energy per chain is the sum of the interfacial tension and the increase in stretching free energy. The phase diagram as a function of the volume fraction is then determined by the crossings of the minimized free energies for each structure (lamellar, bicontinuous cubic, cylindrical, and spherical). These minimized free energies are found to depend on the volume fraction and a parameter, ϵ, the degree of asymmetry which is defined as $\epsilon = (n_A/n_B)(l_A/l_B)^{1/2}$, where n_A and n_B are the number of A and B arms and $l = V/R^2$, where V and R are the volume and the radius of gyration of each arm in the copolymer ($l_{PI}/l_{PS} \sim 0.87$ at 140°C. The predicted phase diagram is shown in Fig. 6.

The morphologies observed for the A_2B and A_3B miktoarm copolymers seem to be in fairly good agreement with those theoretically predicted with the above treatment, at least on a qualitative level. It is seen in the phase diagram that for the A_3B miktoarm copolymers the spherical structure must not be expected in the high PS content region, which confirms the experimental findings. It is also predicted that the triconnected cubic structures should be expected at around 50 vol% PS.

In the case of linear tetrablocks and inverse starblock copolymers, the aim of the study was to produce an architecturally induced transition from one morphology to another at a 50 vol% fraction [11]. All the samples are characterized by an asymmetry parameter which is defined as the ratio between the outer and the inner block molecular weights. The asymmetry parameter values are 1, 2, and 4 (Table 2). It is common knowledge that block copolymers form a lamellar morphology at a wide range of compositions around 50%. This indicates the tremendous stability of this structure. We observed a transition from lamellar to bicontinuous cubic morphology in the case of inverse starblock samples as the asymmetry parameter increased to a value of 4.

The characterization of the bicontinuous cubic structure observed in the inverse starblock copolymers was initially carried out with TEM and SAXS. Unfortunately, the decreased long-range order of the sample did not allow structure
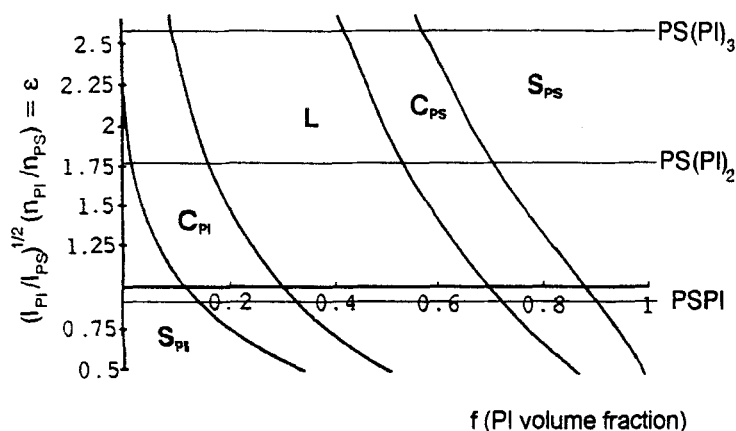

FIG. 6.   Theoretical phase diagram as a function of the volume fraction.

determination with SAXS. We employed image simulations of the strongest candidates of bicontinuous structures in block copolymers: the ordered bicontinuous double diamond structure (OBDD) [12] and the gyroid [13]. For these two structures we constructed a theoretical model for the 50 vol% fraction structure and, by using the appropriate software, we simulated the TEM projections of this structure along the high symmetry directions. Since both morphologies have a cubic symmetry, their high symmetry directions are the (100) (4-fold axis), the (111) (3-fold axis), and the (110) (2-fold axis). For the next step we compared the simulated projections of the two candidate structures with TEM micrographs of the sample which presented projections of the structure along the same directions. Comparison in both real and Fourier space showed that the inverse starblock copolymer's structure is most consistent with the OBDD morphology. The main difference between the OBDD and the gyroid is that the projection along the 2-fold symmetry axis has different symmetries for these two structures (it is p2mm for the OBDD and c2mm for the gyroid).

Finally, we examined the bulk morphology of bridged copolymers of the Super-H type [14]. The characterization of the morphology of these polymers is not yet complete, but the first results indicate new cubic structures.

CONCLUSION

By using anionic polymerization and the chlorosilane approach, the synthesis of model nonlinear block copolymers was made possible. These new materials exhibit interesting morphological features either by moving the borders of the classic phase diagram or by forming new microdomain structures.

ACKNOWLEDGMENTS

REFERENCES

[1]   Y. Tselikas and N. Hadjichristidis, To Be Published.
[2]   H. Iatrou, E. Saikali-Kioulafa, N. Hadjichristidis, J. Roovers, and J. W. Mays, *J. Polym. Sci., Polym. Phys. Ed., 33*, 1925 (1995).
[3]   Y. Tselikas and N. Hadjichristidis, To Be Published.
[4]   H. Iatrou, A. Avgeropoulos, and N. Hadjichristidis, *Macromolecules, 27*, 6232 (1994).
[5]   J. Roovers and P. Toporowski, *Ibid., 14*, 1174 (1981).
[6]   G. E. Molau, in *Block Copolymers* (S. L. A. Agarwal, Ed.), Plenum, New York, NY, 1970.
[7]   F. S. Bates and G. H. Fredrickson, *Annu. Rev. Phys. Chem., 41*, 525 (1990).
[8]   N. Hadjichristidis et al., *Macromolecules, 26*, 5812 (1993).
[9]   Y. Tselikas, H. Iatrou, and N. Hadjichristidis, Submitted.

[10]   S. T. Milner, *Macromolecules, 27*, 2333 (1994).
[11]   Y. Tselikas, N. Hadjichristidis, and E. L. Thomas, Submitted.
[12]   E. L. Thomas, D. B. Alward, D. J. Kinning, D. C. Martin, D. L. Handlin, and L. J. Fetters, *Macromolecules, 19*, 2197 (1986).
[13]   H. A. Hajduk, P. E. Harper, S. M. Gruner, C. C. Honeker, G. Kim, E. L. Thomas, and L. J. Fetters, *Ibid., 27*, 4063 (1994).
[14]   N. Hadjichristidis and E. L. Thomas, Unpublished Results.